

Ultrafast image categorization *in vivo* and *in silico*

Jean-Nicolas Jérémie^{1,†} , Laurent U Perrinet^{2,*} 

¹ Aix Marseille Univ, CNRS;jean-nicolas.jeremie@univ-amu.fr

² Aix Marseille Univ, CNRS;laurent.perrinet@univ-amu.fr

Abstract: Humans are able to categorize images very efficiently, in particular to detect very rapidly the presence of an animal. Recently, deep learning algorithms have achieved higher accuracy than humans for a large set of visual recognition tasks. However, the tasks on which these artificial networks are usually trained and evaluated are usually very specialized which do not generalize well, for example with an accuracy drop following a rotation of the image. In this regard, biological visual systems are more flexible and efficient than artificial systems for more generic tasks, such as detecting an animal. To further the comparison between biological and artificial neural networks, we retrained the standard VGG16 convolutional neural network (CNN) on two independent tasks that are ecologically relevant to humans: detecting the presence of an animal or an artifact. We show that retraining the network achieves a human-like level of performance, comparable to what is reported in psychophysical tasks. Moreover, we show that categorization is better when combining the models' outputs. Indeed, animals (e.g. lions) tend to be less present in photographs containing artifacts (e.g. buildings). Furthermore, these re-trained models were able to reproduce some unexpected behavioral observations of human psychophysics, such as robustness to rotations (e.g., an upside-down or tilted image) or to a grayscale transformation. Finally, we quantified the number of CNN layers needed to achieve such performance, showing that good accuracy for ultrafast image categorization could be achieved with only a few layers, challenging the belief that image recognition would require a deep sequential analysis of visual objects. We hope to extend this framework to bio-mimetic deep neural architectures designed for ecological tasks but also to guide future model-based psychophysical experiments which would deepen our understanding of biological vision.

Keywords: vision, ultrafast animal categorization, deep learning, transfer learning, computational neuroscience, behavior, image categorization, timing

Citation: Jean-Nicolas Jérémie;
Laurent U Perrinet Ultrafast image
categorization *in vivo* and *in silico*.
Vision **2022**, *1*, 0. <https://doi.org/>

Received:

Accepted:

Published:

Publisher's Note: MDPI stays neutral with regard to jurisdictional claims in published maps and institutional affiliations.

Copyright: © 2022 by the authors. Submitted to *Vision* for possible open access publication under the terms and conditions of the Creative Commons Attribution (CC BY) license (<https://creativecommons.org/licenses/by/4.0/>).

1. Introduction

1.1. Biological vision and ultrafast image categorization

What differentiates an image containing an animal from one without? This question of “animacy detection” is crucial for the survival of species, and more specifically in the interactions between preys and their respective predators. This constraint has therefore profoundly shaped the way biological visual systems are processing the retinal input. Of particular importance is the fact that this response must be efficient and rapid, while keeping energy requirements to a minimum. In addition, these systems must fit the ecological niche of the system under consideration, with the image dataset being different for example for a lion, a bird or a human. It is important to note that this biologically inspired approach has similarities and differences with detection algorithms defined in computer vision, and our goal in this paper is both to propose ultrafast image categorization models but also to better understand how biological visual systems can implement them [1].



Figure 1. In ultrafast image categorization [2], the task is to report, for instance by pressing or not a button, if a briefly flashed image (presentation time of the order of 80 ms) contains or not one class of object, for instance an animal, or an artifact. We show here representative images for distractors and targets for each of the “animal” and “artifact” tasks. Note that these tasks are *a priori* independent and that an animal target can either be a target or a distractor for the other task. Here, based on Rousselet *et al.* [3], we did not consider the human being as an animal because it seems to represent a class of its own .

Therefore, let us first define the task of rapidly detecting an animal in a scene (see Figure 1). This task is a routinely used task in the study of biological vision in the lab (for a review, see [4]). In its simplest form, it consists of reporting whether an image contains an animal. Applied to generic natural scenes, the task is such that the animal species is arbitrary, for example birds, a swarm of insects or mammals. Another difficulty is due to the wide variations in identity, shape, pose, size, and position of animals that might be present in the scene. Yet, biological visual systems are capable of efficiently performing such detection in images that are briefly flashed, a so-called tachistoscopic presentation, with a differential activity in electroencephalogram (EEG) recordings in as little as 120 ms for humans [2] or in as little as 80 ms for monkeys [5]. It was also observed in the differential activity of single neurons in the primate lateral prefrontal cortex [6].

This task can be performed with high accuracy (in general with over 80% correct responses), very quickly [7] and robustly to geometric transformations [3]. Color seems to be of little effect yet some low-level statistics [8], as well as other factors (such as the position and size of the animal in the scene) may influence accuracy but not speed [9]. Accuracy is maximal when the animal is in the center of the visual field [10], yet performance is still above chance level (at about 60%) at extreme eccentricities of about 70°. Surprisingly, once the task is learned, novel images are processed as fast as familiar ones [11]. The ultrafast image categorization task and the corresponding recordings are open available from different authors, see for instance [12]. With respect to the difficulty of modeling this task, a scientific question is to understand which features in the image configuration are sufficient to produce an effective behavioral response [13].

1.2. Feed-forward models of ultrafast image categorization

Now that we have defined the computational task, an open question is how to design the best algorithm to solve ultrafast image categorization. First, we can anticipate that there should be a tradeoff between accuracy and speed for image categorization algorithms [14]. In the particular case of ultrafast image categorization and their possible implementation in biological systems, there is a major constraint related to the limits of axonal transduction speed. In humans, for example, an input image evokes activity in the retina after a few milliseconds, and this activity will need about 50 ms to reach the primary visual cortex and another 50 ms before the first motor response can be formed [15]. This leads to major difficulties in modeling the system [16] and is the cause of many visual illusions, such as the flash-lag effect [17]. A first consequence is that the response must be open-loop, that is, before the action can have an effect, for example by triggering a saccadic eye movement [7,18]. A second consequence is that, since the overall process most certainly involves several processing steps, the flow of information is predominantly feed-forward, that is, before recurrent loops can refine neural activity [19]. This was confirmed by EEG recordings of humans performing the task, showing that top-down signals (such as context or expectations) can influence categorization, but that this process is a bottom-up, feed-forward process [20].

In this perspective, it has been shown previously that a feedforward architecture may be sufficient to perform such a task [21]. This architecture consists of a sequence of linear and nonlinear processing layers, similar to the simple and complex cells observed in the primary visual cortex. The linear part of the processing is performed by a convolutional operator, hence the name convolutional neural networks (CNN) for this class of architectures. In these architectures, resolution generally becomes progressively coarser in the higher layers of the hierarchy until a few classification layers lacking a topographic retinotopic structure provides the final output. The efficiency of this model yielded results comparable to humans performing the task on the same images. Other popular methods use oriented luminance gradient histograms [22], but with similar architectures where a sequence of processing steps in image space is followed by a classification step. This mirrors the architecture of the visual system in primates, where the retinal image is transmitted by the thalamus to the primary visual cortex, and then follows a path along the ventral lobe of the cerebral cortex [19].

Architectures similar to [21] have been instrumental in the breakthrough of deep learning architectures, particularly in providing human-like performance for the PASCAL [23] and IMAGENET [24] challenges, that is, for classifying millions of images over 1000 different categories. An important aspect of these architectures, which were initially inspired by neuroscience, is that they can be trained in a supervised manner using gradient descent, as illustrated for the MNIST challenge of classifying handwritten digits [25]. We therefore decided to use them as tools to better understand the process underlying ultrafast categorization of in vivo images while continuing the transfer of knowledge from neuroscience to computer science. Currently, CNNs such as the VGG16 [26] architecture are trained to perform computer domain related tasks, e.g., categorizing the 1000 distinct labels of IMAGENET. Our goal being here to obtain a model faithful to the physiological data, in order to have a reference for comparison, we test this same network on more ecological tasks, such as the recognition of animals or objects in an image (See Figure 2). Unsurprisingly, the performance obtained is very high when the task remains highly computational, but the categorization does not appear to be robust to ecological perturbations such as the rotation of an object of interest (See Figure 2). Yet it is possible to adapt these architectures to solve the categorization of animal images by changing the definition of the supervision pairs and be retrained using the transfer learning method efficiently [27]. The advantage of using such a method is to be able to explore the space of all possible architectures by adapting the synaptic weights of the convolutional kernels but also by testing the meta-parameters of the CNNs, such as the number of layers, the number of

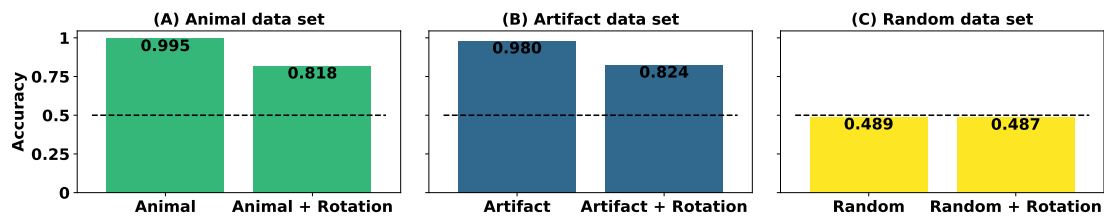


Figure 2. Bar graph representing the accuracy of the VGG network (A) on the data set build with the ‘animal’, (B) build with the ‘artifact’ synset or on the control ‘random’ data set [33] (see Methods 2.1). The network is tested with the raw images (left) or after applying a random rotation (right). The dotted line represents the chance level for all graphs.

channels in each layer, or the coarsening of the visual information along the hierarchy [28], in order to obtain the most coherent and ecological model possible.

One drawback of these networks is their lack of interpretability, yet their raw efficiency gives a lower bound to the possibility of solving a given task. In the extreme case, one can expect that even the best CNN network will be unable to learn to categorize an image-independent feature, for example, whether the calendar day on which the photo was taken is even or odd. We will show in the following that if we define a task that consists of random labels among the 1000 categories of IMAGENET, then none of our architectures can learn the task efficiently. The situation is different when defining more ecological tasks such as animal or artifact detection. Searching for this type of categories seems to be a primordial feature of the brain [19]. For example, it has shown that convolutional neural networks trained with a blurred-to-focused image training sequence can reveal fundamental differences between the processing of faces and objects [29]. Such a method can also be used by changing the definition of the supervision pairs to study changes in task context and investigate rapid categorization and interference of objects in the image [30]. In summary and somewhat counter-intuitively, it may therefore be more difficult to make a binary choice such as detecting an animal in an image than to select from 1000 labels, and this paper will allow us to better understand how this is achieved, both *in vivo* and *in silico*.

1.3. Main contributions

To answer this scientific question, our paper proposes three major contributions. First, in order to define the psycho-physical task, we will build a large dataset of images based on IMAGENET [24]. It is defined by selecting labels according to a large semantic graph of English words: WORDNET [31] (see Figure 3). As a control task, we will also define an independent task, which consists in detecting the presence of any artifact in the image (see Figure 1 (B)). Second, we will re-train an existing CNN on these tasks and compare its performances with experimental data. This will allow us to test the robustness of our networks against several geometric transformations and to compare their accuracy with those observed in the physiological data. Moreover, we will compare the accuracy for both tasks, individually or jointly. Third, we will test different levels of complexity of such models by performing a gradual removal of layers from the original network. Such an experiment will quantify whether low level features may be sufficient to categorize animals [32] and also whether this is accompanied by a decrease in the invariance to geometrical deformations. Finally, we will discuss how this work can be beneficial for the design of physiological experiments and in the design of new architectures for computer vision.

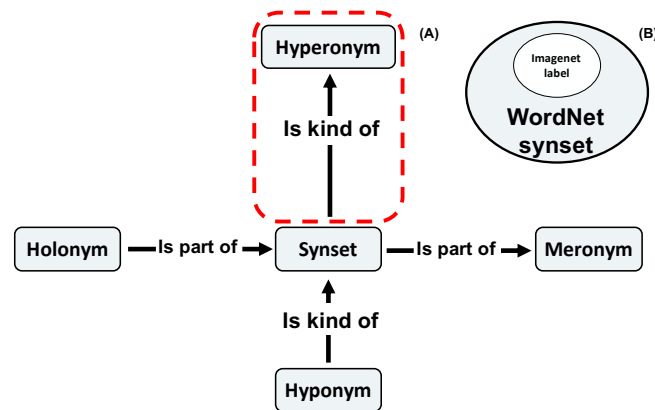


Figure 3. (A) Schematic displaying the different semantic links between the synsets of the WORDNET network. We focused on the hyperonym link (frame in red) to build datasets from IMAGENET synsets, for instance, which are 'kind of' an 'animal'. (B) Venn diagram exposing the subset of IMAGENET label included in the WORDNET synset's set.

2. Methods

2.1. Dataset maker using WORDNET hierarchy

To train a deep convolutional network (like VGG 16) on a specific task, one of the most important components is the data set. We needed a tool that allows us to generate data sets fit to answer our question. Therefore we made a library which from a keyword produces a dataset with image folders containing (target) or not this keyword (distractor) [33]. For example, if we set the data set maker with the keyword 'animal', since the set of labels from the IMAGENET database [24] is based on a large lexical database of the English language: WORDNET [31], the nouns, verbs, adjectives, and adverbs in this database are grouped into a graphical set of cognitive synonyms: synset, each expressing a distinct concept. These synsets are linked between them by employing a few conceptual relationships (see Figure 3). We used the hyperonym link to detect, for instance, that a German shepherd is one kind of dog and that a dog is one kind of 'animal', thus defining a hyperonym path. In that example, the 'animal' WORDNET'S synset is in the hyperonym path of the 'German shepherd' IMAGENET's label. Based on this relation, the data set maker selected a specific subset of labels in the IMAGENET database to build our data sets. Once the list of labels corresponding to our task is selected, the data set maker randomly chooses from the URLs provided for IMAGENET challenge [24] to download the images forming the dataset. We generated three datasets with the dataset maker: A dataset based on the synset 'animal' and a dataset based on the synset 'artifact'. We also made a 'random' dataset generated by randomly selecting 500 labels of the IMAGENET database. The latter was generated to infer in the role of the semantic link between labels in the efficiency of the categorization by a deep convolutional network.

Using this tool, we generate datasets corresponding to a given task. In particular, by choosing the 'animal' synset, we generated the dataset necessary to train the network answering our question "is there an animal in this scene?". We followed the same protocol to answer the question "is there an artifact in this scene?". Each newly build dataset contains a 'train', 'validation' and 'test' folder (with, respectively 1200, 800 and 2000 images). Each folder contains a 'target' and a 'distractor' category (with equal numbers of images). All networks are trained on the 'train' folder and tested during their learning on the corresponding 'validation' folder. Then, we compute the accuracies using the 'test' folder. As a control, we tested the networks on the dataset of Serre *et al.* [21] which contains a total of 600 targets (images containing an animal) and 600 distractors (images not containing an animal).

2.2. Transfer Learning

We use the transfer learning method to re-train networks [27]. This method takes advantage of the knowledge gained on one task to transfer it to a different but related task. Here, we use an existing network pre-trained on a specific task: the VGG16 [26]. This architecture is taken from the PYTORCH [34] library and trained on the IMAGENET database to solve the IMAGENET [24] challenge. We previously found that this model offered the best trade off between efficiency and more complex characteristics like the Brain score [35], since we want to model biological function. Compared to other architectures such as ResNet, the VGG16 stands out as the best candidate [36].

Two notable advantages of this method are the robustness and speed of convergence of the network, which results in lower total running time and energy consumption. In particular, this method allows us to save computational time during the learning process and thereby experiment with several possible strategies (see Figure 4). We first test this hypothesis by training a network with random weights: VGG NAIVE as a control.

During transfer learning, we kept all layers of the network VGG16 because it is already capable of performing feature extraction on natural scenes, and re-trained the last fully connected layer. In particular, we replaced this last layer trained on IMAGENET (thus with a vector of dimension $K = 1000$ which captures the predicted probability of detection for each of the labels in the IMAGENET database), with a layer with an output dimension of $K = 1$ representing the predicted probability for the detection of a new object of interest, i.e., a target and not a distractor. We then re-trained this fully connected layer, while freezing the weights of the other layers, to match the pre-trained features (the output of the convolutional layers) with the synset corresponding to the new task implemented by the dataset maker. As a control, we also tested the effectiveness of freezing the remaining layers by completely re-training all layers of the pre-trained network, VGG FULL.

When training the network, since the network makes a binary choice ("is this synset present in this scene"), we implement the loss using the binary cross-entropy loss with logits from the PYTORCH library. We used the Stochastic Gradient Descent (SGD) optimizer of the PYTORCH library and validated parameters such as batch size, learning rate, momentum by performing a scan of these parameters for each network. During the sweep, we vary one of these parameters over a given range while the others are held at the default value (batch size = 16, learning rate = 0.0001, momentum = 0.9) for 5 epochs. We choose the value that gives the best average accuracy on the validation set.

To increase the generality of our results, we implemented various preprocessing steps on the inputs. In particular, we applied the Auto-augment function from the PYTORCH library to warp the input images. This function implements a total of 16 randomly parameterized affine transformations on the inputs to perform data augmentation [37], thus defining our main re-training network: VGG GEN. We tested the effectiveness of this data augmentation by re-training a pre-trained network with a set of custom transformations from the PYTORCH library, random horizontal flipping (with $p=0.5$), random vertical flipping (with $p=0.5$), and random gray scale (with $p=0.5$): VGG CUSTOM. Finally, we test these protocols to quantify the role of these variations during the training process on the accuracy of the network.

2.3. Pruning

Another network manipulation we will test is to modify the CNN architecture. In particular, we will test the effect of pruning the convolutional layers of the pre-trained network VGG16 to determine the complexity of the features that are required to categorize a given synset of interest. Indeed, one may describe the VGG16 network as a hierarchically organized pipeline: first a set of convolutional layers, then a set of fully connected layers. The set of convolutional layers is organized into 5 blocks of 13 convolutional layers. Within a block, there is a sequence

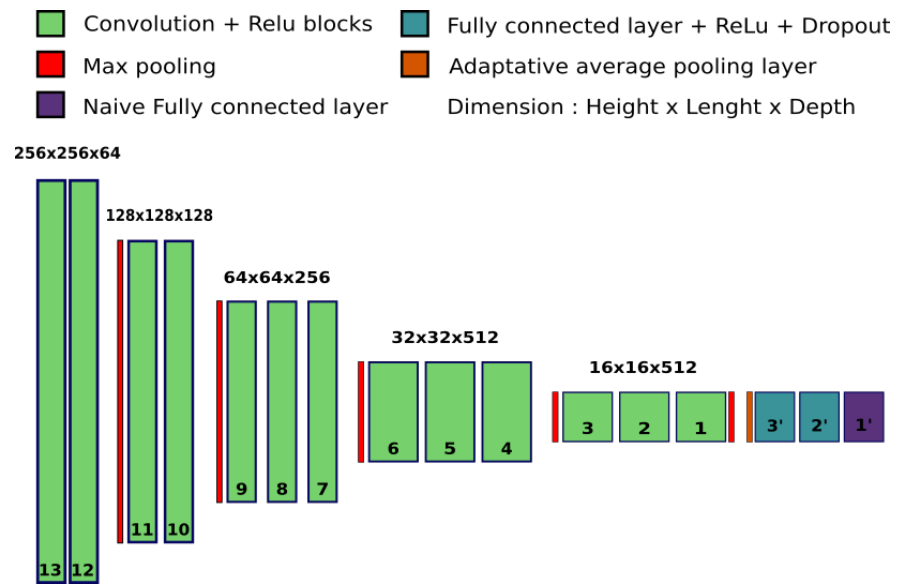


Figure 4. A diagram of the network architecture used in transfer learning. In green, the 5 blocks of 13 convolutional layers noted from 13, at the entrance, to 1, at the junction with the fully connected part here represented in blue and purple. The purple layer represents the naive layer substituting the one in the Pytorch architecture.

of convolutional layers followed by a nonlinearity and optionally a normalization (in our case, we do not use or test the batch normalization option). In each individual block, the image size and the number of channels are constant. In general, the resolution decreases from block to block using max-pooling operations, while the number of channels increases from 64×64 at the input to 512×512 at the fully connected blocks).

Since the final process of the set of convolutional layers is an adaptive pooling function that produces a characteristic image of constant size equal to 7×7 , the size and architecture of the fully connected layers will be held constant. We therefore define new networks whose names correspond to the number of layers that are pruned. The network named VGG-1 has its last 512×512 convolutional layers pruned, and then we apply the same learning process as used for the network VGG GEN. We then proceed in a similar way for the 12 different depth factors (from the deepest VGG-1 to the shallowest VGG-12).

2.4. Accuracy

As a generic measure of performance, we evaluated the accuracy of our different networks on the test set. This metric is typically used to describe the performance of the model. Effectively, the network is expected to output a binary choice ('is there an animal in the scene?') and is designed to provide the predicted probability of the presence of a synset of interest in the scene. We considered the output as 'target' if the network output is greater than .5 (i.e. 50%), otherwise it was considered as a 'distractor'. Then, a Positive True is defined in the event that the network categorizes a 'target' when it is a 'target', otherwise it defines a Positive False. Similarly, a True Negative is the case where the network categorizes a 'distractor' when it is indeed a 'distractor', otherwise it defines a False Negative. Based on these observations, we can determine each time that the networks performed a good categorization and calculate its accuracy as the ratio of the sum of True Positives and Negatives over the total number of tested samples. In order to provide a comparison with the state of the art, we tested the VGG IMAGENET and computed its prediction by summing the predictions of the labels belonging to

dataset build with dataset maker, Synset: Animal						
	IMAGENET	Naive	Full	Gen	Custom	
Accuracy	0.995	0.667	0.939	0.947	0.956	
dataset from Serre <i>et al.</i> [21]						
	IMAGENET	Full	Gen	Custom	Serre et al's model	Human
Accuracy	0.96	0.91	0.89	0.90	0.84	0.80

Table 1. Mean accuracies for the ultrafast image categorization of an animal in a scene from a newly build dataset using our library dataset maker with the synset 'animal' (top) or for the Serre *et al.* [21] dataset (bottom) for different transfer learning strategies.

the hyperonymous path of the synsets of interest after the softmax layer. The accuracy is then computed following the same methodology as for the re-trained networks.

$$\text{Accuracy} = \frac{\text{True}_{\text{positive}} + \text{True}_{\text{negative}}}{\text{True}_{\text{positive}} + \text{True}_{\text{negative}} + \text{False}_{\text{positive}} + \text{False}_{\text{negative}}} \quad (1)$$

Equation 1 used to get the accuracy of the networks based on their outputs.

3. Results

3.1. Performances on natural scenes containing animals

First, we test different variations of transfer learning on the task "Is there an animal in this visual scene?" and display the mean accuracies for different datasets. First, the VGG IMAGENET network seems efficient in the categorization on our newly build dataset as it reach a 99.5% mean accuracy. Also, the latter seems robust as on the dataset used by Serre *et al.* [21] on which the network obtains a 96% mean accuracy. Note that it reaches better performances compared to those obtained by the model designed in Serre *et al.* [21] (about 84%) and neurophysiological data (about 80%) (see Table 1) without any re-training process. Now let's focus on the network after the learning process, as the VGG FULL, VGG CUSTOM and VGG GEN reach even performances on the test set (with 94.7%, 95.6% and 93.9% respectively) and also keep a robust categorization on Serre *et al.* [21] dataset (with 96%, 90% and 89% respectively). Compared with the VGG NAIVE which could only reach 66.7% on the same task, these results show that transfer learning allows us to get highly accurate networks for the categorization of a synset of interest with a slight loss in the accuracy compared with the original networks on this particular task. Now we will focus on the robustness of the categorization of the different transfer learning strategies (VGG FULL, VGG CUSTOM and VGG GEN) compared with the state of the art VGG IMAGENET and the expected performance in neurobiological models.

3.2. Robustness of the categorization with different geometric transformations

Since they are the networks that obtain the best performance for this task, we tested the robustness of VGG GEN, VGG CUSTOM and VGG IMAGENET on the newly constructed dataset using our dataset maker library with the synset 'animal'. We applied either a gray scale filter, a vertical or a horizontal reflection on the input (see Table 2). We also test the robustness to rotation by rotating the image around the center by an angle ranging from -180° to $+180^\circ$ (see Figure 5). All these networks maintain good average accuracy on the returned data set and on the gray scale dataset (see Table 2). These surprising results are in agreement with

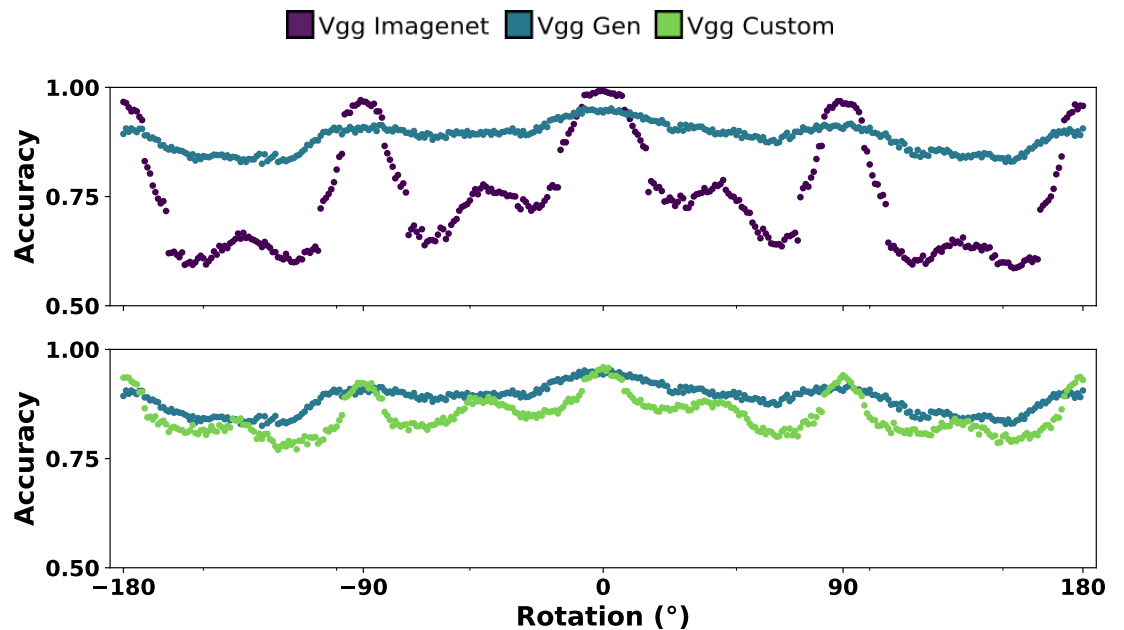


Figure 5. Average accuracy on the test dataset of re-trained networks for different rotations of the input image. (Top) the VGG IMAGENET displayed with the VGG GEN networks. (Bottom) the VGG GEN displayed with the VGG CUSTOM networks. The rotation is applied around the center with an angle ranging from -180° to $+180^\circ$.

psychophysical results showing that ultrafast categorization is robust in grayscale images [2]. Only VGG GEN appears to show robust accuracy at all angles with peaks in accuracy at cardinal orientation (-180° , -90° , 0° , 90° , and 180°), these could be explained by the pre-training weights of the networks as they correspond to the peaks found in the categorization of VGG IMAGENET. We conclude here that, overall, transfer learning provides a more robust categorization of the synset of interest by the network, as the VGG GEN, VGG CUSTOM achieve better performance in this task. In addition, the protocol used to re-train the network VGG GEN, with the Autoaugment function of the library PYTORCH [37], is also better than custom data augmentation (details in Methods). Therefore, by its stability, the robustness of categorization to different image transformations of VGG GEN is similar to that reported in psychophysics [3]. The performance of VGG GEN is very close to that of VGG FULL with a tendency for VGG GEN to be more robust to rotation. We will therefore focus on the features that this model relies on to perform its categorization.

3.3. Dependence of accuracy scores between the two tasks

First examined the influence of the objects of interest on the learning performance of VGG GEN by introducing a variation of the synset of interest in the construction of the data set. We used our "data set maker" tool with the keyword 'artifact', thus generating a new network trained to categorize the presence of the 'artifact' synset in a natural scene: VGG ARTIFACT. We display the average accuracy of the networks trained to detect the animal synset (here VGG ANIMAL stand for our VGG GEN) on the dataset constructed with the 'animal' synset (respectively trained to detect the artifact synset tested on the dataset constructed with the artifact synset). Next, we tested the networks trained to detect the 'animal' synset on the dataset constructed with the 'artifact' synset and vice versa. Here, by exposing the predictions for the 'animal' and 'artifact' synsets, we highlight a bias in the composition of the dataset. Although

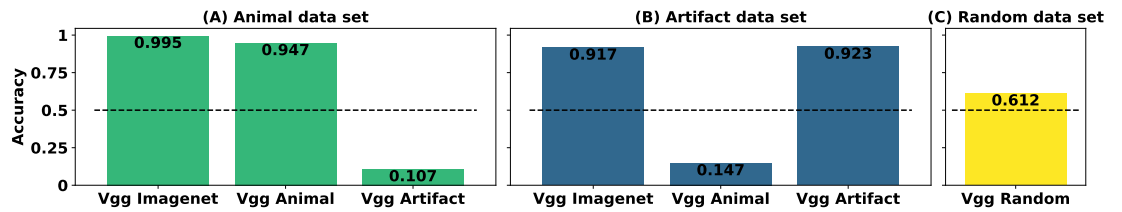


Figure 6. Bar graph representing the accuracy of VGG IMAGENET, VGG ANIMAL and VGG ARTIFACT networks (A) on the data set build with the "animal" synset or (B) build with the "artifact" synset. (C) display the mean accuracy of the VGG RANDOM network on the corresponding data set (see Methods 4). The dotted line represents the chance level for all graphs.

the outputs are independent, the 'animal' images confidently match the 'non-artifact' images (and vice versa), thus facilitating global detection (see Figure 6).

Incidentally, this bias is also present in the dataset used by Serre *et al.* [21]. Yet, when we compare the performance of the humans on this dataset with the performance achieved by the network on a frame-by-frame basis, we found a high correspondence (about 84%) in their correct predictions. Indeed, for some images, the networks failed in categorization, but the human succeeded and vice versa. For some images, both the network and the human succeed or fail in categorizing an animal (see Figure 7). We have displayed images where one human or both a human and our model failed to categorize an animal in the scene, as this may reflect the specific features that humans or our models rely on to perform their categorization. This close relationship between human and network responses could allow us to select images and design physiological tests to extract the features necessary for such detection.

As a control, we tested the VGG RANDOM network on the corresponding dataset (see Subsection 2.1 for details). As it obtains an average accuracy close to the one obtained with the VGG NAIVE network, its poor performance can be explained by the fact that the pre-trained weights of the VGG IMAGENET network do not match the new task.

3.4. What features are necessary to achieve the task?

We designed an experiment in which we gradually remove layers from a pre-trained network VGG16 for 12 different "depth" factors. For each level, we test the re-trained pruned networks to categorize an animal in a scene on our dataset IMAGENET. VGG GEN achieves the best accuracy for this task, with a slight drop at VGG-1, followed by a plateau phase between VGG-1 and VGG-8. Then, another drop occurs between VGG-9 and VGG-12 where the networks settle close to the chance level (see Figure 8). The accuracies of the networks remain similar to the performance found by Serre *et al.* [21]. This is not a surprise as their model relies on low-level features [32]. Note that the computational time required to perform the categorization decreases with the accuracy of the network (in seconds on a GTX1080 GPU, we obtain VGG GEN = 0.005 ± 0.0001 , VGG-8 = 0.003 ± 0.0001).

We also tested all the pruned networks on our IMAGENET dataset by rotating the image around the center from -180° to $+180^\circ$, the categorization can lose robustness with fewer layers (see Figure 9). Indeed, as the number of layers and the average accuracy decrease, the standard deviation increases (VGG GEN = 88.62 ± 3.13 , VGG-8 = 73.50 ± 5.36). Although the networks appear to be able to categorize an animal with fewer layers, they seem to trade this temporal advantage by their robustness to transformations such as rotations.

In order to get a better idea of the size of the features needed to categorize an animal in a scene, we finally test the networks on a new "shuffled" dataset, where the image has been subdivided into square patches of varying sizes and then blended to generate a new image [38]. Since CNN networks are by definition robust to translations, patch translation should not interfere with categorization unless it breaks some necessary patterns in the images. With few

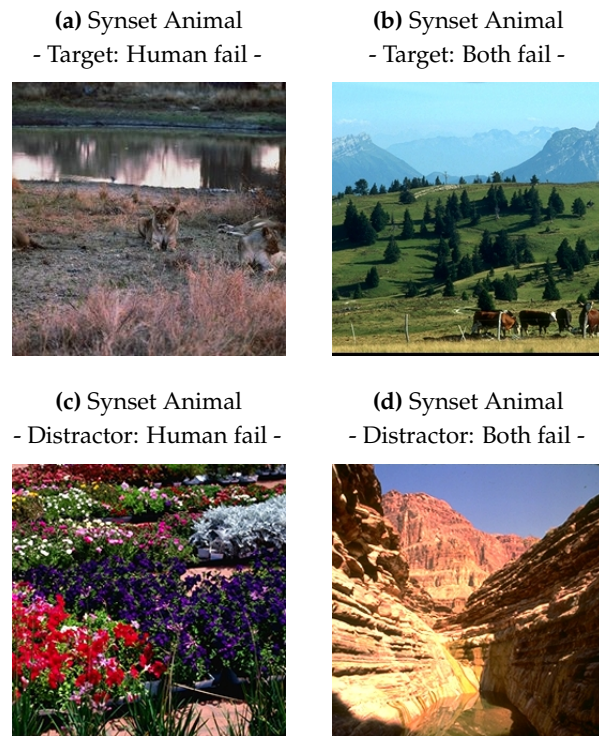


Figure 7. Some prototypical example images where either (a) Humans failed to categorize an animal in a scene but our model succeeds, (b) Humans and our model both failed to categorize an animal in the scene, (c) Human failed to categorize the absence of animal in a scene but our model succeed, (d) Human and our model failed to categorize the absence of animal in the scene. The psychophysical data and the images are taken from the dataset used by Serre *et al.* [21]

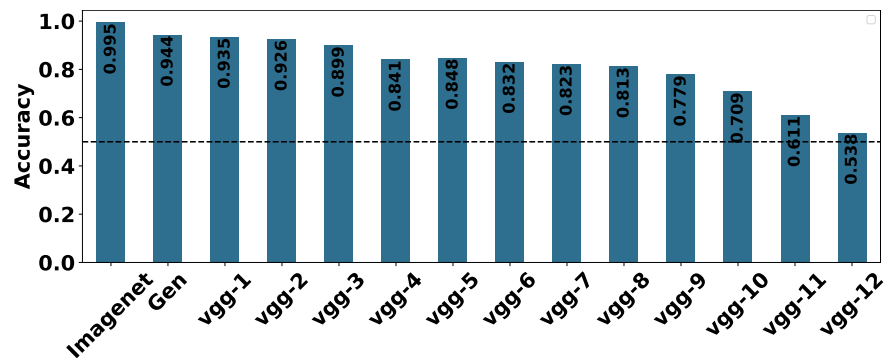


Figure 8. Average accuracy obtained as a function of depth in pruning networks. The networks are re-trained to categorize animals and tested on test datasets based on IMAGENET images constructed using the 'animal' synset. The next subscript "vgg-" indicates the number of convolutional layer blocks pruned from the original network (see Subsection 2.3 for more details). The dotted line represents the chance level for all graphs.

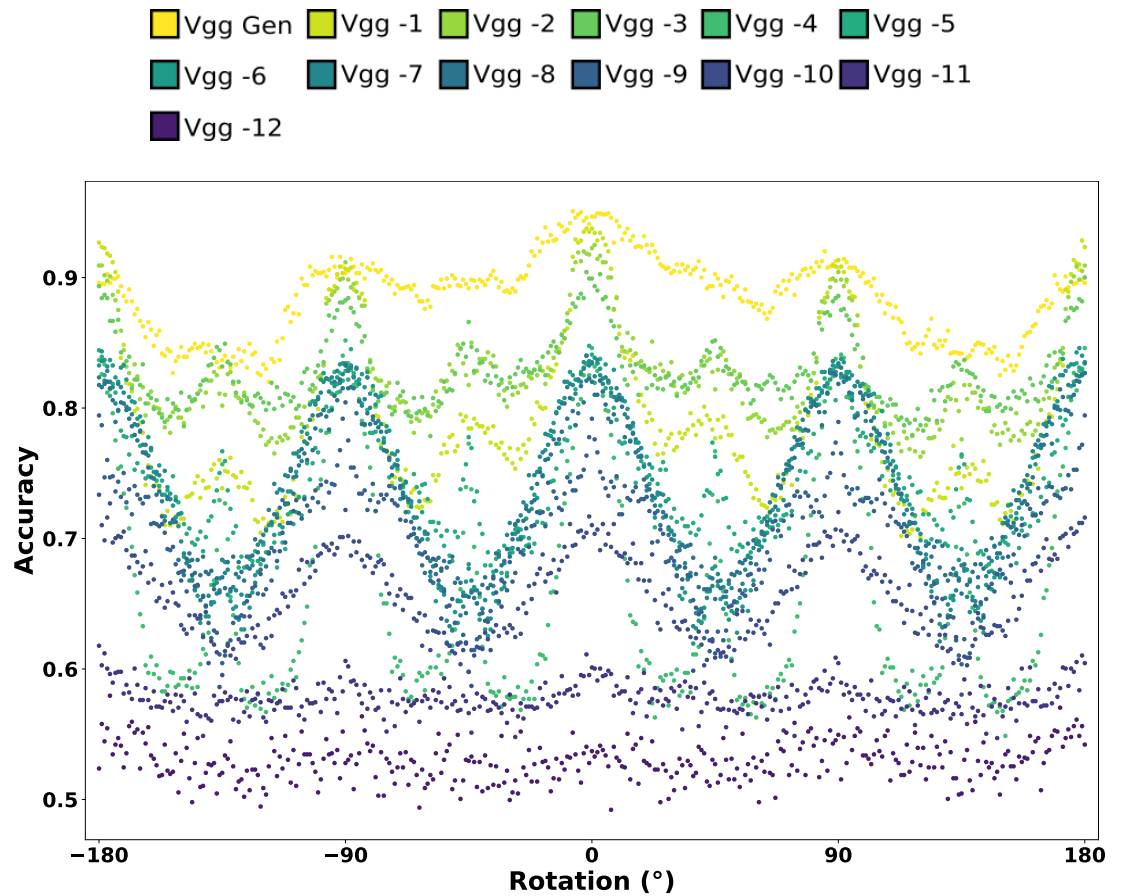


Figure 9. Average accuracy over the test dataset of the re-trained networks for rotations around the center from -180° to $+180^\circ$. These networks were tested on a dataset based on IMAGENET images constructed using the 'animal' synset. The index following "vgg-" indicates the number of convolutional layers pruned on the networks (with vgg-1 the deepest and vgg-12 the shallowest).

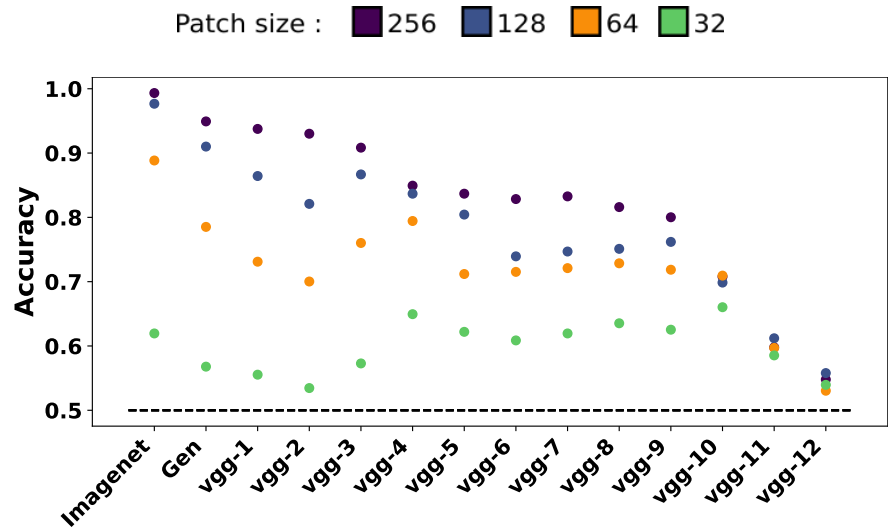


Figure 10. Mean accuracy obtained for the differentially pruned networks over the ‘shuffled’ test dataset in which we use a shuffled transformation on the input image. We show the results as we decrease the size of the shuffled patches on the images. The networks were re-trained to categorize animals and tested on datasets based on IMAGENET images built using the ‘animal’ synset. The index following “vgg-” indicates the numbers of convolutional layers pruned on the networks. The dotted line represents the chance level for all graphs.

layers the networks should rely on low level features to perform its categorization, indeed we get an idea of the size of features necessary for different deepness. In fact, between patch sizes 256×256 and 64×64 , the categorization of the networks is robust to this transformation (see Figure 10). But as soon as we reach the size of 32×32 pixels, the accuracy of all networks drops sharply. Furthermore, there seems to be a transition between deeper networks and medium-sized networks, as the latter obtain better average accuracies for this task. So the size of the features needed to perform such a task varies with the depth of the network. For example, VGG GEN appears to use feature sizes between 32×32 and 64×64 pixels, as its accuracy drop when we pass this threshold (see Figure 10), but further study is needed to quantify this size. In a future application, we could extract features from these low-level layers to better understand the features needed to perform this task. This would allow us to design a stimulus set for a psychological task as in Thorpe *et al.* [2]. Such a test could be relevant to whether these features are sufficient to categorize an animal in a flashed scene.

4. Discussion

In this paper, we have shown that we may re-train networks using transfer learning to apply it on an ecological task. These networks achieve accuracies similar to those found in psycho-physical responses in humans. Furthermore, the robustness of the categorization is comparable to that found in psycho-physical data. In particular, we have shown quantitatively that the categorization of the re-trained networks may be robust to transformations such as rotations, reflections or grayscale filtering, such as is observed in humans [2,3].

Two independent networks each re-trained on each of the two categorization tasks brought to light a link, or rather a bias in this categorization. This kind of bias is also found in humans and seems to impact the categorization as well [39]. The question of detecting an animal in an image is indeed tightly linked to that of detecting an artifact, putting in the shade the possibility of the less likely appearances of an animal object (like a teddy bear) or of a non-animal non-object (like a mountain). The study of this kind of bias could possibly allow

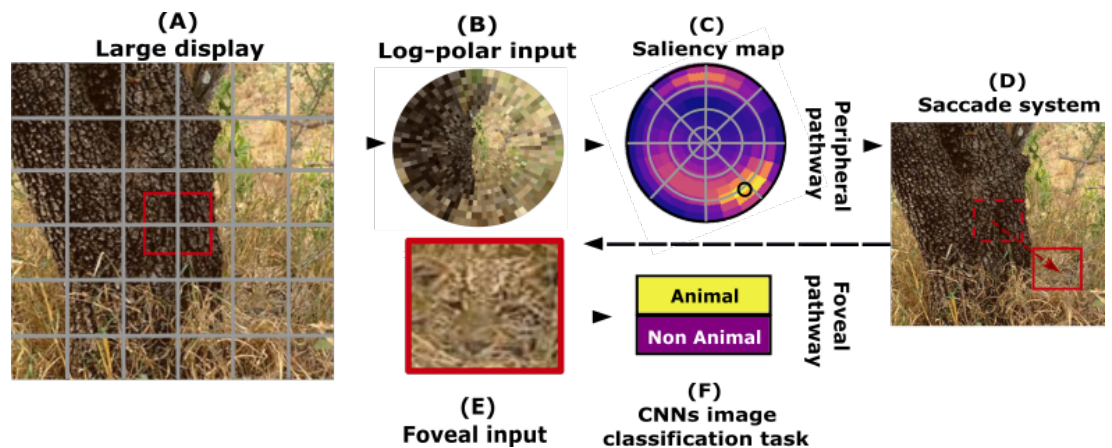


Figure 11. Model build over the anatomical visual processing pathways observed in mammals, namely the “What” and the “Where” pathways: Peripheral pathway (top row) is applied to a large display from a natural scene (A): It is first transformed into a retinotopic log-polar input (B) and we then learn to return a “saliency map” (C). The latter infers, for different positions in the target, the predicted accuracy value that can be reached by the foveal pathway, mimicking the “Where” pathway used for global localization. The position with the best accuracy will feed a saccade system (D), adjusting the fixation point at the input of the foveal pathway (bottom row). It takes a subsample (E) of the large display (A), over which a categorization is done (F), mimicking the “What” pathway.

building ecologically-relevant datasets to maximize the learning process of the networks in order to discover more about the features needed for categorization.

Even if the level of 80% of correct categorization correspond between human and machine in this kind of task, they could be driven to make different “mistakes”, and these particular examples could then be used as subjects of studies in the design of psycho-physical tests. Moreover, these systematic errors could be a window to shed light on some processes in our understanding the visual pathways of primates. The last part of our study was based on the search for the features necessary for categorization. We obtain that, in agreement with the studies conducted by Serre *et al.* [21], a simple feed-forward network based on low level features is sufficient to perform efficiently the categorization. Moreover, we can estimate the size of the features needed around 32×32 pixels and 64×64 pixels. Although the categorization is still possible at this very low computational cost, it loses in robustness.

5. Perspectives

One of the main goals of this study was to provide a comparison on an ecological and well studied task used in primate visual neuroscience. Although this study focuses on the analysis of categorization, it is a necessary step for a well-known task in the field of vision: visual search. This task consists of the simultaneous localization and detection of a visual target of interest. Applied to the case of natural scenes, searching for example for an animal (either a prey, a predator or a partner) constitutes a challenging problem due to large variability over numerous visual dimensions. Previous models managed to solve the visual search task by dividing the image into sub-areas. This is at the cost, however, of computer-intensive parallel processing on relatively low-resolution image samples [40,41]. Taking inspiration from natural vision systems [42], we develop here a model that builds over the anatomical visual processing pathways observed in mammals, namely the “What” and the “Where” pathways [43]. It operates in two steps, one by selecting a region of interest, before knowing their actual visual content, through an ultrafast/low resolution analysis of the full visual field, and the second providing a detailed categorization over the detailed “foveal” selected region

attained with a saccade (see Figure 11). Modeling this dual-pathways architecture allows offering an efficient model of visual search as active vision. In particular, it allows filling the gap with the shortcomings of CNNs with respect to physiological performances. In the future, we expect to apply this model to better understand visual pathologies in which there would exist a deficiency of one of the two pathways [44] while contributing to the field of computer vision.

Data Availability Statement: This work is made reproducible using the following tools. First the code reproducing all figures is available on [GitHub](#) [?] and in particular the code of [DataSetMaker](#) [33] used to retrieve images.

The paper is available as an [arXiv preprint](#) with links to previous versions and to the code. Find also the associated [zotero group](#) used to regroup relevant literature on the subject.

Acknowledgments: Authors received funding from the ANR project number ANR-20-CE23-0021 (“[AgileNeuroBot](#)”). For the purpose of open access, the author has applied a CC BY public copyright licence to any Author Accepted Manuscript version arising from this submission.

Conflicts of Interest: The authors declare no conflict of interest.

Abbreviations

(D)CNN	(Deep) Convolutional Neuronal Network
VGG	Vision Geometry Group
MNIST	Modified or Mixed National Institute of Standards and Technology

References

1. Cristóbal, G.; Perrinet, L.U.; Keil, M.S. *Biologically Inspired Computer Vision*; Wiley-VCH Verlag GmbH and Co. KGaA: Weinheim, Germany, 2015-10-07, 2015. <https://doi.org/10.1002/9783527680863>.
2. Thorpe, S.; Fize, D.; Marlot, C. Speed of Processing in the Human Visual System. *Nature* **1996**, *381*, 520–522. <https://doi.org/10.1038/381520a0>.
3. Rousselet, G.A.; Macé, M.J.M.; Fabre-Thorpe, M. Is It an Animal? Is It a Human Face? Fast Processing in Upright and Inverted Natural Scenes. *Journal of Vision* **2003**, *3*, 440–455. <https://doi.org/10.1167/3.6.5>.
4. Fabre-Thorpe, M. The Characteristics and Limits of Rapid Visual Categorization. *Frontiers in Psychology* **2011**, *2*. <https://doi.org/10.3389/fpsyg.2011.00243>.
5. Fabre-Thorpe, M.; Richard, G.; Thorpe, S.J. Rapid Categorization of Natural Images by Rhesus Monkeys. *Neuroreport* **1998**, *9*, 303–308. <https://doi.org/10/fbrdkh>.
6. Freedman, D.J.; Riesenhuber, M.; Poggio, T.; Miller, E.K. Categorical Representation of Visual Stimuli in the Primate Prefrontal Cortex. *Science* **2001**, *291*, 312–316. <https://doi.org/10.1126/science.291.5502.312>.
7. Kirchner, H.; Thorpe, S.J. Ultra-Rapid Object Detection with Saccadic Eye Movements: Visual Processing Speed Revisited. *Vision Research* **2006**, *46*, 1762–1776. <https://doi.org/10.1016/j.visres.2005.10.002>.
8. Mirzaei, A.; Khaligh-Razavi, S.M.; Ghodrati, M.; Zabbah, S.; Ebrahimpour, R. Predicting the Human Reaction Time Based on Natural Image Statistics in a Rapid Categorization Task. *Vision Research* **2013**, *81*, 36–44. <https://doi.org/10/f4szpd>.
9. Zhu, W.; Drewes, J.; Gegenfurtner, K.R. Animal Detection in Natural Images: Effects of Color and Image Database. *PloS One* **2013**, *8*, e75816. <https://doi.org/10.1371/journal.pone.0075816>.
10. Thorpe, S.; Fabre-Thorpe, M. Seeking Categories in the Brain. *Science (New York, N.Y.)* **2001**, *291*, 260–263. <https://doi.org/10/bzn42k>.
11. Fabre-Thorpe, M.; Delorme, A.; Marlot, C.; Thorpe, S. A Limit to the Speed of Processing in Ultra-Rapid Visual Categorization of Novel Natural Scenes. *Journal of Cognitive Neuroscience* **2001**, *13*, 171–180. <https://doi.org/10/dghjvt>.
12. Delorme, A. Go-NoGo Categorization and Detection Task **2021**. <https://doi.org/10.18112/OPENNEURO.DS002680.V1.2.0>.
13. Crouzet, S.M. What Are the Visual Features Underlying Rapid Object Recognition? *Frontiers in Psychology* **2011**, *2*. <https://doi.org/10.3389/fpsyg.2011.00326>.
14. Delorme, A.; Richard, G.; Fabre-Thorpe, M. Key Visual Features for Rapid Categorization of Animals in Natural Scenes. *Frontiers in Psychology* **2010**, *1*.
15. Macé, M.J.M.; Joubert, O.R.; Nespoulous, J.L.; Fabre-Thorpe, M. The Time-Course of Visual Categorizations: You Spot the Animal Faster than the Bird. *PLoS ONE* **2009**, *4*, e5927. <https://doi.org/10.1371/journal.pone.0005927>.
16. Perrinet, L.U.; Adams, R.A.; Friston, K.J. Active Inference, Eye Movements and Oculomotor Delays. *Biological Cybernetics* **2014-12-16**, **2014**, *108*, 777–801. <https://doi.org/10.1007/s00422-014-0620-8>.

17. Khoei, M.A.; Masson, G.S.; Perrinet, L.U. The Flash-Lag Effect as a Motion-Based Predictive Shift. *PLOS Computational Biology* **2017**, *13*, e1005068. <https://doi.org/10.1371/journal.pcbi.1005068>.
18. Yarbus, A. Eye Movements during the Examination of Complicated Objects. *Biofizika* **1961**, *6*(2), 52–56.
19. Thorpe, S.J.; Gegenfurtner, K.R.; Fabre-Thorpe, M.; Bülthoff, H.H. Detection of Animals in Natural Images Using Far Peripheral Vision. *The European Journal of Neuroscience* **2001**, *14*, 869–876. <https://doi.org/10.1046/j.0953-816x.2001.01717.x>.
20. Delorme, A.; Rousselet, G.A.; Macé, M.J.M.; Fabre-Thorpe, M. Interaction of Top-down and Bottom-up Processing in the Fast Visual Analysis of Natural Scenes. *Brain Research. Cognitive Brain Research* **2004**, *19*, 103–113. <https://doi.org/10.1016/j.cogbrainres.2003.11.010>.
21. Serre, T.; Oliva, A.; Poggio, T. A Feedforward Architecture Accounts for Rapid Categorization. *Proceedings of the National Academy of Sciences of the United States of America* **2007**, *104*, 6424–6429. <https://doi.org/10/cr3ksx>.
22. Rangdal, M.B.; Hanchate, D.B. Animal Detection Using Histogram Oriented Gradient. *International Journal on Recent and Innovation Trends in Computing and Communication* **2014**, *2*, 7.
23. Everingham, M.; Eslami, S.M.A.; Van Gool, L.; Williams, C.K.I.; Winn, J.; Zisserman, A. The PASCAL Visual Object Classes Challenge: A Retrospective. *International Journal of Computer Vision* **2015**, *111*, 98–136. <https://doi.org/10.1007/s11263-014-0733-5>.
24. Russakovsky, O.; Deng, J.; Su, H.; Krause, J.; Satheesh, S.; Ma, S.; Huang, Z.; Karpathy, A.; Khosla, A.; Bernstein, M.; et al. ImageNet Large Scale Visual Recognition Challenge. *International Journal of Computer Vision (IJCV)* **2015**, *115*, 211–252. <https://doi.org/10.1007/s11263-015-0816-y>.
25. Lecun, Y.; Bottou, L.; Bengio, Y.; Haffner, P. Gradient-Based Learning Applied to Document Recognition. *Proceedings of the IEEE* **Nov./1998**, *86*, 2278–2324. <https://doi.org/10.1109/5.726791>.
26. Simonyan, K.; Zisserman, A. Very Deep Convolutional Networks for Large-Scale Image Recognition. *arXiv:1409.1556 [cs]* **2015**, [[arXiv:cs/1409.1556](https://arxiv.org/abs/1409.1556)].
27. Yosinski, J.; Clune, J.; Bengio, Y.; Lipson, H. How Transferable Are Features in Deep Neural Networks? **2014**. <https://doi.org/10.48550/arXiv.1411.1792>.
28. Cichy, R.M.; Khosla, A.; Pantazis, D.; Torralba, A.; Oliva, A. Comparison of Deep Neural Networks to Spatio-Temporal Cortical Dynamics of Human Visual Object Recognition Reveals Hierarchical Correspondence. *Scientific Reports* **2016**, *6*, 27755. <https://doi.org/10.1038/srep27755>.
29. Jang, H.; Tong, F. Convolutional Neural Networks Trained with a Developmental Sequence of Blurry to Clear Images Reveal Core Differences between Face and Object Processing. *Journal of Vision* **2021**, *21*, 6. <https://doi.org/10.1167/jov.21.12.6>.
30. Joubert, O.R.; Rousselet, G.A.; Fize, D.; Fabre-Thorpe, M. Processing Scene Context: Fast Categorization and Object Interference. *Vision Research* **2007**, *47*, 3286–3297. <https://doi.org/10/b467m6>.
31. Fellbaum, C., Ed. *WordNet: An Electronic Lexical Database*; Language, Speech, and Communication, A Bradford Book: Cambridge, MA, USA, 1998.
32. Perrinet, L.U.; Bednar, J.A. Edge Co-Occurrences Can Account for Rapid Categorization of Natural versus Animal Images. *Scientific Reports* **2015**, *5*, 11400. <https://doi.org/10/gdj5wj>.
33. Jérémie, J.N. Data Set Maker, 2022.
34. Paszke, A.; Gross, S.; Massa, F.; Lerer, A.; Bradbury, J.; Chanan, G.; Killeen, T.; Lin, Z.; Gimelshein, N.; Antiga, L.; et al. PyTorch: An Imperative Style, High-Performance Deep Learning Library. In *Advances in Neural Information Processing Systems 32*; Wallach, H.; Larochelle, H.; Beygelzimer, A.; dAlché-Buc, F.; Fox, E.; Garnett, R., Eds.; Curran Associates, Inc., 2019; pp. 8024–8035.
35. Schrimpf, M.; Kubilius, J.; Hong, H.; Majaj, N.J.; Rajalingham, R.; Issa, E.B.; Kar, K.; Bashivan, P.; Prescott-Roy, J.; Geiger, F.; et al. Brain-Score: Which Artificial Neural Network for Object Recognition Is Most Brain-Like? *bioRxiv : the preprint server for biology* **2020**, [<https://www.biorxiv.org/content/early/2020/01/02/407007.full.pdf>]. <https://doi.org/10.1101/407007>.
36. Jérémie, J.N.; Perrinet, L.U. Experimenting with Transfer Learning for Visual Categorization. Technical report, Zenodo, 2021. <https://doi.org/10.5281/zenodo.5770069>.
37. Cubuk, E.D.; Zoph, B.; Mane, D.; Vasudevan, V.; Le, Q.V. AutoAugment: Learning Augmentation Policies from Data. *arXiv:1805.09501 [cs, stat]* **2019**, [[arXiv:cs, stat/1805.09501](https://arxiv.org/abs/1805.09501)].
38. Biederman, I. Perceiving Real-World Scenes. *Science (New York, N.Y.)* **1972**, *177*, 77–80. <https://doi.org/10.1126/science.177.4043.77>.
39. Bogadhi, A.R.; Buonocore, A.; Hafed, Z.M. Task-Irrelevant Visual Forms Facilitate Covert and Overt Spatial Selection. *The Journal of Neuroscience: The Official Journal of the Society for Neuroscience* **2020**, *40*, 9496–9506. <https://doi.org/10.1523/jneurosci.1593-20.2020>.
40. Liu, W.; Anguelov, D.; Erhan, D.; Szegedy, C.; Reed, S.; Fu, C.Y.; Berg, A.C. SSD: Single Shot MultiBox Detector. *arXiv:1512.02325 [cs]* **2016**, *9905*, 21–37, [[arXiv:cs/1512.02325](https://arxiv.org/abs/1512.02325)]. https://doi.org/10.1007/978-3-319-46448-0_2.
41. Ren, S.; He, K.; Girshick, R.; Sun, J. Faster R-CNN: Towards Real-Time Object Detection with Region Proposal Networks. *arXiv:1506.01497 [cs]* **2016**, [[arXiv:cs/1506.01497](https://arxiv.org/abs/1506.01497)].
42. Mishkin, M.; Ungerleider, L. Object Vision and Spatial Vision: Two Cortical Pathways. *Trends in Neurosciences* **1983**, *6*, 414–7. <https://doi.org/10/c4kbpn>.

-
43. Daucé, E.; Albigès, P.; Perrinet, L.U. A Dual Foveal-Peripheral Visual Processing Model Implements Efficient Saccade Selection. *Journal of Vision* **2020-06-05**, **2020**, *20*, 22–22. <https://doi.org/10/gg9ccs>.
 44. Wiecek, E.; Pasquale, L.; Fiser, J.; Dakin, S.; Bex, P. Effects of Peripheral Visual Field Loss on Eye Movements During Visual Search. *Frontiers in Psychology* **2012**, *3*. <https://doi.org/10.3389/fpsyg.2012.00472>.

Dataset build with dataset maker, Synset: Animal				
	IMAGENET	Full	Gen	Custom
Vertical flip				
Accuracy	0.956	0.903	0.904	0.943
Horizontal flip				
Accuracy	0.993	0.946	0.953	0.958
Gray scale filter				
Accuracy	0.963	0.929	0.918	0.942

Table 2. Mean accuracies for the ultrafast image categorization of an animal in a scene from a newly build dataset using our library dataset maker with the synset ‘animal’ for three re-trained networks: VGG GEN, VGG CUSTOM and VGG FULL compared with the state of the art network VGG IMAGENET using various geometrics transformation on the input: Vertical flip, Horizontal flip, Gray scale filter. All the transformations used here are performed using the Pytorch library [34]